crystals

MDPI

Review

A Critical Review of Anti-Corrosion Chemical Surface Treatment of Aluminum Alloys Used for Sports Equipment

Bo Leng [1], Yuhua Xue [2], Jing Li [3], Jiantao Qi [4], Aihua Yi [5] and Qixin Zhao [4,*]

1 College of Education, Beijing Sports University, Beijing 100091, China; lbihh@sina.com
2 Marine Chemicals Research Institute, Qingdao 266001, China; xueyuhua163@163.com
3 The Boiler & Pressure Vessel Safety Inspection Institute of Henan Province, Zhengzhou 450003, China; hngj_rsb@163.com
4 College of New Energy, China University of Petroleum (East China), Qingdao 266580, China; jiantao.qi@upc.edu.cn
5 School of Materials Science and Engineering, Dongguan University of Technology, Dongguan 523808, China; yiaihua92751@163.com
* Correspondence: 2015040210@s.upc.edu.cn

Abstract: Aluminum alloys with low-weight property are promising structure materials for sports equipment. Alloying element-rich second-phase particles create the risk of localized corrosion and result in failure of sports equipment. Chromate conversion coatings as conventional and successful surface treatments were employed to provide a thin but compact film against corrosion. However, chromate species were toxic and carcinogenic for human beings and this process has been highly restricted. In this sense, alternative processes such as trivalent chromium conversion coating with low environmental risk require better corrosion-resistant performance compared to chromate conversion coating. In addition, the closed-loop system of the chromate electroplating process has been used in Europe and the United States. This is also a sustainable process for surface treatment of aluminum alloys applied in sports equipment. The present paper aims to summarize the methods and types of different aluminum alloy surface treatments and compiles the effects of various surface treatments on the corrosion resistance of aluminum alloys. The eco-friendly application of aluminum alloys in the field of sports equipment may be facilitated in the future.

Keywords: aluminum alloy; sports equipment; corrosion; surface treatment

Citation: Leng, B.; Xue, Y.; Li, J.; Qi, J.; Yi, A.; Zhao, Q. A Critical Review of Anti-Corrosion Chemical Surface Treatment of Aluminum Alloys Used for Sports Equipment. *Crystals* **2024**, *14*, 101. https://doi.org/10.3390/cryst14010101

Academic Editor: Shouxun Ji

Received: 27 November 2023
Revised: 21 December 2023
Accepted: 23 December 2023
Published: 22 January 2024

1. Introduction

Health-improving sports activities increase enjoyment and quality of life. The popularity of sports activities boosts the ever-increasing demands for improving sports equipment to meet different needs. Athletes desire advanced equipment that can improve their performance. Beginners may wish to employ their equipment more comfortably and easily. Disabled people may hope to use assistive equipment to improve the quality of their life. Application of light alloys as the primary structure materials is the main method to make advanced sports equipment. In terms of light alloys, aluminum alloy with low density and efficient supply outweighs other light alloys (magnesium and titanium alloys, as seen in Figure 1) [1–3]. Alloying elements such as copper, silicon and iron added into the aluminum matrix enhance the mechanical properties (stiffness and strength). This also generates cathodic islands at the aluminum alloy surface, inducing the corrosion initiation in corrosive environments [4,5]. In this sense, surface treatment methods with good corrosion-resistant performance are required in practice [6].

Aluminum alloys show good resistance against corrosion due to the surface oxide of a contact Al_2O_3 film which can block the corrosive ions from the bulk metal surface [7]. Aluminum alloys are favored in many sports such as cycling, golf, tennis, mountaineering

and racing and the internal instrumentation of athletes and equipment precisely because of these advantages.

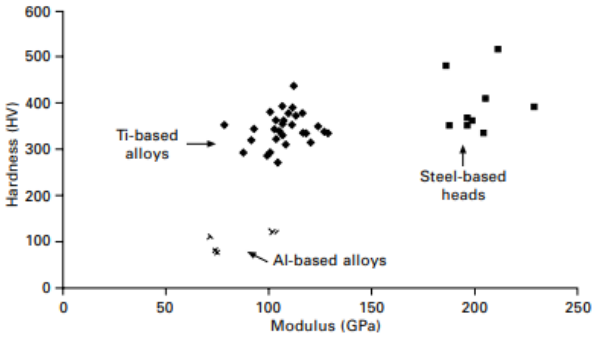

Figure 1. Plot of hardness vs. E for head materials employed in sports equipment [2].

With consideration of the sports environment, human oil, salts and sweat are the main corrosion environments. Sweat with a weak acidic property mainly consists of sodium chloride, influencing the application safety of sports equipment especially regarding long-term service and strong competition sports. Thus, low-density, corrosion-resistant surface treatment is required for sports equipment.

In the present paper, aluminum alloys applied in sports equipment and the related surface treatment with current states and future development are discussed. With consideration of eco-friendliness, the green and sustainable surface treatment of aluminum alloys is the hot spot of research and practice.

2. Types and Properties of Aluminum Alloy Sport Equipment

Application of aluminum alloys in sports equipment started from 1926 and ushered in an explosive period. Table 1 displays the types and properties of aluminum alloys applied in sports and related equipment and instrumentation (+ in the table indicates excellent performance and − indicates poor performance) [8]. High-strength, low-density and highly effectively corrosion-resistant aluminum alloys in sports equipment are always required. For example, the head of a golf club faces impact force of up to 1.47×10^4 N, requiring advanced high-performance Al-Sc aluminum alloys.

Table 1. Types and properties of aluminum alloys applied in sports equipment [8].

Category	Part Name	Al Alloy	Lightweight	Intensity	Hardness	Corrosion Resistance	Abrasion Resistance	Machinability	Appearance
Baseball	Hard baseball bat	7001, 7178	+	+	+	−	−	−	−
	Soft baseball bat	6061, 7178	+	+	+	−	−	−	−
	Ball case	6063, 1050A	+	+	−	+	−	−	+
	Pitching position	1050A	+	+	−	+	−	−	+
Tennis	Racket frame	6061, 2A12, 7046	+	+	−	−	+	+	+
	Racket handle rivet	2A11	+	−	−	−	−	−	−
	Tennis racket hoop	1100	+	−	−	−	−	−	−
Badminton	Badminton racket frame	6061, 2A12	+	+	−	−	+	+	+
	Badminton racket joint	ADC12	+	−	−	−	+	+	+

Table 1. *Cont.*

Category	Part Name	Al Alloy	Lightweight	Intensity	Hardness	Corrosion Resistance	Abrasion Resistance	Machinability	Appearance
Skis	Stressed part	7A09, 7178	+	+	—	—	—	—	—
	Skis edge	7A09, 7178	+	+	—	—	—	—	—
	Rear protection plate	6061	+	—	+	—	+	—	+
	Bevel guard plate	7178	+	—	+	—	+	—	+
	Bottom fender	5A02	+	—	+	—	+	—	+
	Buckle and shell	ADC6, ADC12	+	+	—	+	—	+	—
	Belt structure	ADC6, ADC12	+	+	—	+	—	+	—
Ski pole	Battle itself	6061, 7001, 7178	+	+	+	—	—	—	+
	Retaining ring	6063	+	—	—	—	—	—	—
Arrows	Poles, bows	2A12, 7A09	+	+	—	—	—	—	+
Track and field	Brace, strut, cross bar	6063, 7A09	+	+	—	+	—	—	+
	hurdle	6063, 5A02	+	—	—	+	—	—	+
	Javelin throw	2A12, 7A09	+	+	—	—	—	+	+
	Relay baton	1050A, 5A02	+	—	—	+	—	—	+
	Starter, flare gun	6063, ADC12	+	—	—	+	—	+	+
Hiking trip	Cooking utensils, eating utensils, water bottles	1060, 3003, 5A02	+	—	—	+	—	—	+
	Backpack rack, chair	6063, 7A09	+	+	—	—	—	—	+
Golf	bat	7A09	+	+	—	—	—	—	—
	Parachute column	5A02	+	+	—	+	—	—	—
	Club head box	ADC10, etc.	+	—	—	—	+	—	—
		1050A	+	—	—	—	—	—	—
Fencing	Mask	2A11	+	+	—	+	—	+	+
Hockey puck	racket stick	7A04, 7178	+	+	—	—	—	—	—
Shoes	Running shoes nail nuts	2A11	+	+	—	—	—	—	—
	Ski shoe rivet	2A11	+	+	—	—	—	—	—
	Ski shoe belt buckle	6063	+	—	—	—	+	—	+
	Football shoe bolt	ADC12	+	—	—	—	+	—	+
Bicycle	Various parts	2A14, 2A11, 6061 etc	+	—	—	+	—	+	+
Swimming pool	Side plate, bottom plate	5A02	+	—	—	+	—	+	+
	conduit	3003, 6A02, 6063	+	—	—	+	—	+	+
	Reinforcement parts, pillars	6063	+	—	—	+	—	—	+
Football, water polo, Ice hockey, Rugby	Door, column	6061, 6063	+	+	—	—	+	—	+
Other facilities	Seats, trellises, Changing room	6063 etc	+	—	—	—	+	—	+
Rowing	Mast, boat body	7A19, 5083 etc	+	+	—	+	—	—	—
Dive	Board, rack	6070 etc	+	+	—	+	—	+	+

As seen from Table 1, badminton sports employed AA 6061 and 2A12 alloys for the rackets and ADC12 aluminum alloys as racket joints. Different components and manufacturing methods can distinguish their types as deformed aluminum alloy and cast aluminum alloys. AA 6061 and 2A12 alloys are deformed aluminum alloys and ADC12 aluminum alloys are cast aluminum alloys.

3. Surface Microstructure and Components

Aluminum is remarkable for its favorable properties, for example, the relatively low density and good corrosion resistance due to the phenomenon of passivation. Superpure aluminum, with 99.99% purity, is primarily applied as a reference material in the lab. The mechanical properties of the alloy are improved by the addition of copper, zinc and magnesium. AA 2A12 aluminum alloy (Al-Cu alloy) has been used in a wide range of high-tech applications such as in the aircraft industry, defense components and badminton rackets. Its nominal composition is 3.8~4.9% Cu, 1.2~1.8% Mg, 0.3~0.9% Mn, with lesser amounts of Fe, Si and impurity elements. In comparison with AA 2A12 aluminum alloys, AA 6061 alloys (Al-Mg-Si alloy) with the main components of 0.8–1.2 wt.% Mg, 0.4–0.8 wt.% Si, 0.15–0.4 wt.% Cu alloying elements display high strength and good weldability and formability. The superior mechanical properties of these two deformed aluminum alloys are required for the high quality of badminton rackets. In addition, ADC12 aluminum alloys, as cast aluminum alloys, contain the main alloying components of 9.6–12 wt.% Si and 1.5–3.5 wt.% Cu. These cast aluminum alloys with good formability are employed as the racket joint [9–11].

Material microstructure is a main influence on the corrosion property. Microstructural heterogeneities are present in aluminum alloys, especially in formed and cast aluminum alloys, with major consideration given to the distribution of intermetallic particles.

Alloy casting is an important processing procedure in which alloying and impurity elements are added to change the material properties. Coarse intermetallic compounds, formed interdendritically by eutectic decomposition during the ingot solidification, can be classified into two groups: insoluble intermetallic compounds and soluble intermetallic compounds. The former usually contain the impurity elements iron or silicon, and examples include Al_6(Fe, Mn), Al3Fe, α-Al(Fe, Mn, Si) and Al_7Cu_2Fe. The latter, as equilibrium intermetallic compounds of the major alloying elements, consist of Al_2Cu, Al_2CuMg and Mg_2Si. Lacy networks are formed in both types of particles surrounding the cast grains. Preheating or ingot homogenization is helpful to dissolve the soluble compounds. In the meantime, the subsequent fabrication of the cast ingots helps to fracture the remaining particles and make them aligned in the direction of metal flow. The main second-phase particles in AA2xxx include Al_2Cu, Mg_2Si, $Al_{12}Si$(Mn, Fe), Al_2CuMg, Al_3(Mn, Fe) and Al_6(Mn, Fe).

It has been shown that the wear resistance of aluminum alloys depends on the depth of penetration of the abrasive material, and Figure 2a,b shows the abraded material at large grain sizes. It can be clearly observed that the grain size is large, and for alloys subjected to higher loads, the larger the abrasive grain size, the higher the wear rate [12]. Buchheit et al. [13] showed that approximately 60% of intermetallic particles with dimensions greater than 0.7 μm are S-phase (Al_2CuMg) with their fraction corresponding to 2.7% of the total surface area. Moreover, $(Al, Cu)_x(Fe, Mn)_ySi$, such as modified forms of Al_8Fe_2Si or $Al_{10}Fe_2Si$ type IMCs, is suggested as the base composition of AA2024 by Gao et al. [14]. Hughes et al. [15,16] investigated a minimum of nine separate compositions including the matrix and at least one periphery zone around S-phase/θ-phase composite particles by means of a state-of-the-art electron microprobe. They found the composition difference was in both S-phase/θ-phase composite particles and the matrix, in which the former can be decomposed into smaller domains of S-phase and θ-phase. Furthermore, most cathodic particles contained Si similar to the research of Gao et al. [14]. Al_6(CuFeMn) particles are suggested as only one component amongst the cathodic particles without Si, which is similar to the report of Hughes et al. [15,16]. Shell-shaped particles were reported by

Campestrini and co-workers in AA2024 alloy after a long quench delay time [17]. However, differences in their chemical compositions exist between the core and the outer layer. The same elements are found in both the bulk of the shell-shaped particle and irregular shaped Al-Cu-Mn-Fe-(Si) particles. Aluminum, copper and magnesium mainly contribute to the shell, and α-phase particles are generally accepted to be the Al-Cu-Mn-Fe-(Si) type IMCs in the present study.

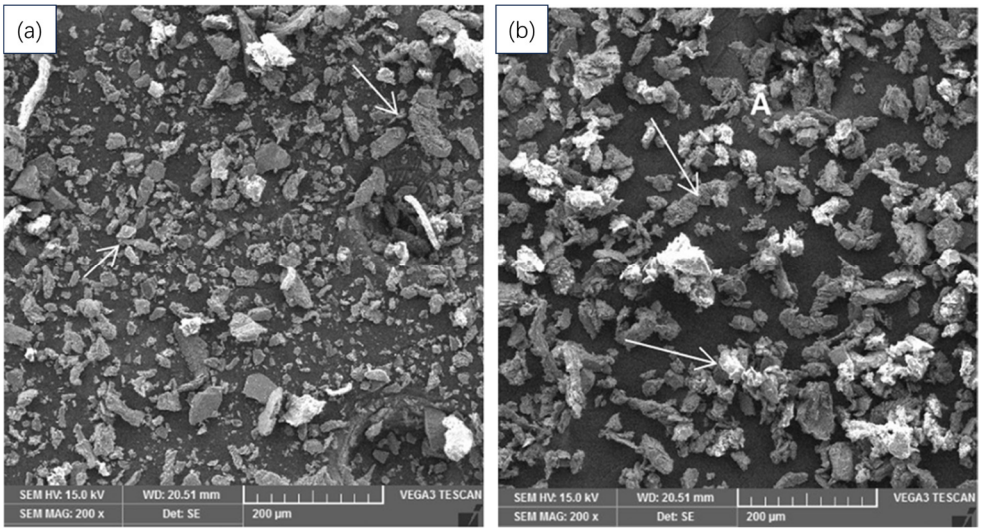

Figure 2. Worn surfaces of (**a**) Al 6082 alloy operated at larger grit size and (**b**) Al 6082/SiC/Gr composite operated at larger grit size [12].

Dispersoids (typically 0.05–0.5 µm) form during homogenization of the aluminum ingots by solid state precipitation. The elements of intermetallic compounds show modest solubilities and slow diffusion rates in solid aluminum. It is easy for an aluminum alloy to develop these particles, such as $Al_{20}Mn_3Cu$, $Al_{12}Mg_2Cr$ and Al_3Zr, which resist dissolution and coarsening and retard recrystallization and grain growth during processing and heat treatment.

In dilute Al-Sc, Al-Zr and Al-Sc-Zr alloys, precipitation of L12-Al3X dispersions leads to dispersion strengthening and improved high-temperature stability [18]. In AA2024-T3 aluminum alloy, a homogeneous dispersoid distribution was found in the matrix except for the periphery of Al_2CuMg particles by Wang et al. [19]. An $Al_{20}Mn_3Cu_2$ dispersoid-free zone surrounds the coarse intermetallic particles. In truth, the formation of S-phase particles, which are rich in copper, results in a preferential depletion of copper in the matrix around them. This is not advantageous to precipitation of dispersoids, because the dispersoids are also copper-containing intermetallic compounds. Franc et al. showed that the addition of 0.15–0.25 wt.% Zr promotes the formation of Al3Zr dispersions in AA 6086 alloy, which reduces grain growth during homogenization and solution treatment and improves grain strengthening [20].

Fine precipitates (up to 0.1 µm) form during age hardening (e.g., AA2A12). In terms of the Al-Cu-Mg alloys, S-phase (Al_2CuMg) precipitate formation is well studied because of the significance for strengthening of AA2xxx aluminum alloy. The S-phase preferentially nucleates on dislocations and dislocation loops as an agglomerate form during precipitation from solid solution. Finally, individual nano-scale particles develop with a homogeneous distribution for the form of S-phase in the matrix [21]. The alloys AA 6086 and AA 6082 were analyzed as an example. The main difference between the two alloys is the silicon, copper and zirconium content. AA 6082 has a silicon content of 0.7–1.3 wt.%, while AA 6086 has a silicon content of 1.3–1.7 wt.%. The higher the silicon content in the alloy, the higher the percentage of magnesium- and silicon-based precipitates in the microstructure. An increase in copper content from 0.1% to 0.8 wt.% copper (0–0.1 wt.% copper in AA

6082) promotes the formation of copper-rich precipitates, which improves the precipitation hardening effect [20].

4. Surface Morphology

Freshly abraded aluminum and its alloys immediately develop a thin alumina oxide film when exposed to near-neutral environments. The thickness of this film present on superpure aluminum is approximately 2 nm [22]. In terms of the grown oxide film structure, various investigations have been carried out with different proposed structures. For instance, Wilsdorf's experimental results show the effect on the structure of a large excess of aluminum ions (existing in <50 Å thin film), which are amorphous and at the same time have a strong reflection characteristic of crystalline γ-Al_2O_3, with a rather imperfect long-range order development [23].

Moreover, this thin film with residual and mechanical flaws is not a "perfect" corrosion barrier on the aluminum alloy due to the existence of non-metallic inclusions, second-phase particles, impurity and grain boundaries. The pitting corrosion initially develops at the imperfection and active flaws of the oxide film in corrosive environments, for example, a solution containing chloride ions.

The hydration of air-formed film has different characteristics primarily depending on the temperature. Between 60 °C and 70 °C, Hart [24] suggested that this film growth in water proceeds in three stages: (1) "amorphous", (2) boehmite, γ-$Al(OH)_3$ and (3) bayerite, β-$Al(OH)_3$, the final film thus consisting of three layers. During the formation of an amorphous oxide at 25 °C, the major aluminum monomer species varies with pH in the following fashion: Al^{3+} for pH < 3, $Al(OH)^{2+}$ for pH 4–5, $Al(OH)^{2+}$ for pH 5–6 and $Al(OH)^{4-}$ for Ph > 6.5. So, the temperature and pH value are key parameters that influence the composition of the amorphous oxides [25].

5. Corrosion

Corrosion in aluminum-based sport equipment happens due to the corrosive working environment such as human oil. In terms of corrosion type, surface morphologies were employed for the corrosion categorization and it includes pitting, intergranular corrosion and stress-induced corrosion cracking.

Pitting or pit corrosion is typical localized corrosion and the alloying second-phase particles at the surface are the initiation site. As shown in Figure 3, Yang et al. [7] employed an O_2 gas environment transmission electron microscope to investigate the surface oxide during deformation at room temperature. They revealed the liquid-like and self-healing aluminum oxide present at the aluminum surface and it determined the corrosion resistance.

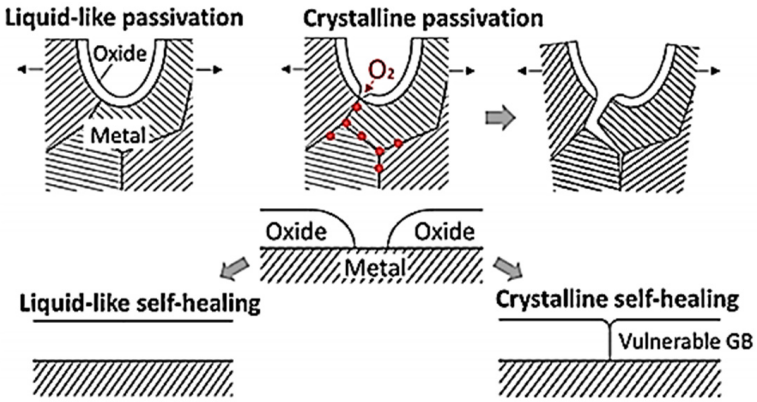

Figure 3. Schematic diagram of the self-healing process of aluminum oxide at room temperature [7].

With consideration of magnesium alloying elements in high-strength aluminum alloys, intergranular corrosion is prone to occur in corrosive environments. As shown in Figure 4,

Wei et al. [26] employed a scanning electron microscope and SEM ultamicrotome (GATAN 3View) to reveal the magnesium-rich precipitates resulting in the severe sensitization of AA 5083 alloy in a marine environment.

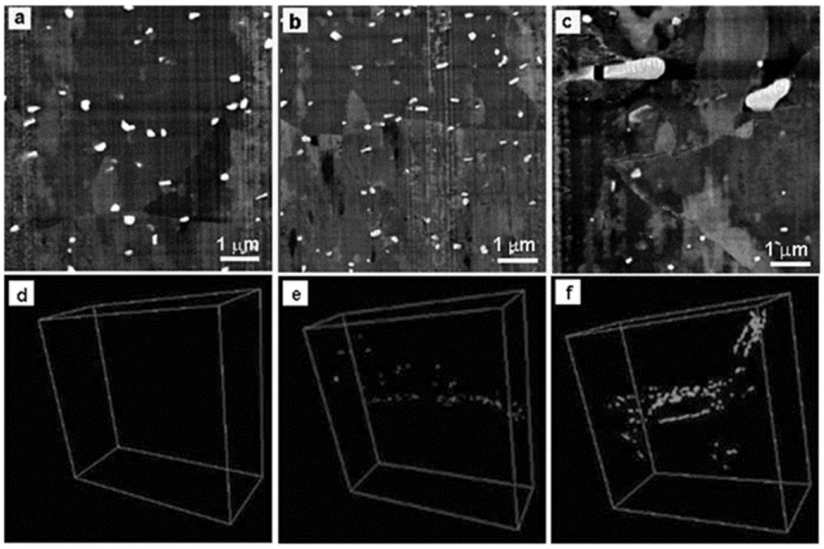

Figure 4. Schematic diagram of the self-healing process of aluminum oxide at room temperature, (**a**–**c**) SEM images of representative regions from the center of the alloy plate; and (**d**–**f**) corresponding 3D reconstructions with transparency applied to the alloy matrix and clear spots applied to Mg-rich precipitates [26].

In addition, Zhang et al. [27] employed electrochemical measurement and a scanning electron microscope to reveal the transition from intergranular corrosion to crystallographic pitting in AA 2024-T351 aluminum alloys in 3.5 wt.% NaCl solutions as shown in Figures 5 and 6. Second-phase particles, especially as Al-Cu phase, revealed the corrosion crevices (as seen in Figure 6d) when aluminum alloys experience polarization close to the breakdown potential, marked as "Stage 2" (as seen in Figure 5). In comparison, the surface and particles displayed a negligible effect by the increasing voltage up to "Stage 1".

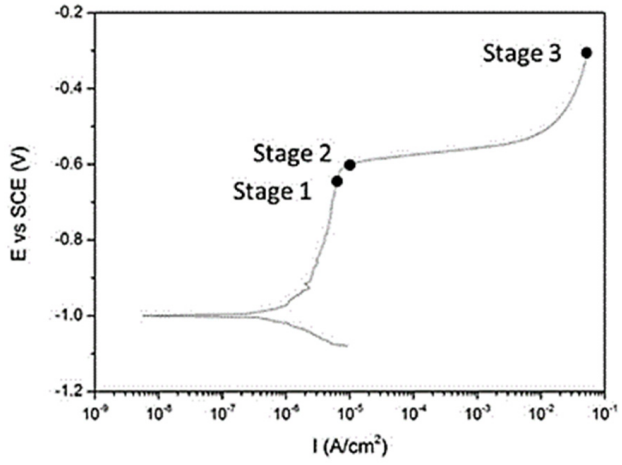

Figure 5. Potential–current density curve of the AA2024-T351 aluminum alloy during the potentiodynamic polarization in a de-aerated 3.5 wt% NaCl solution at ambient temperature [27].

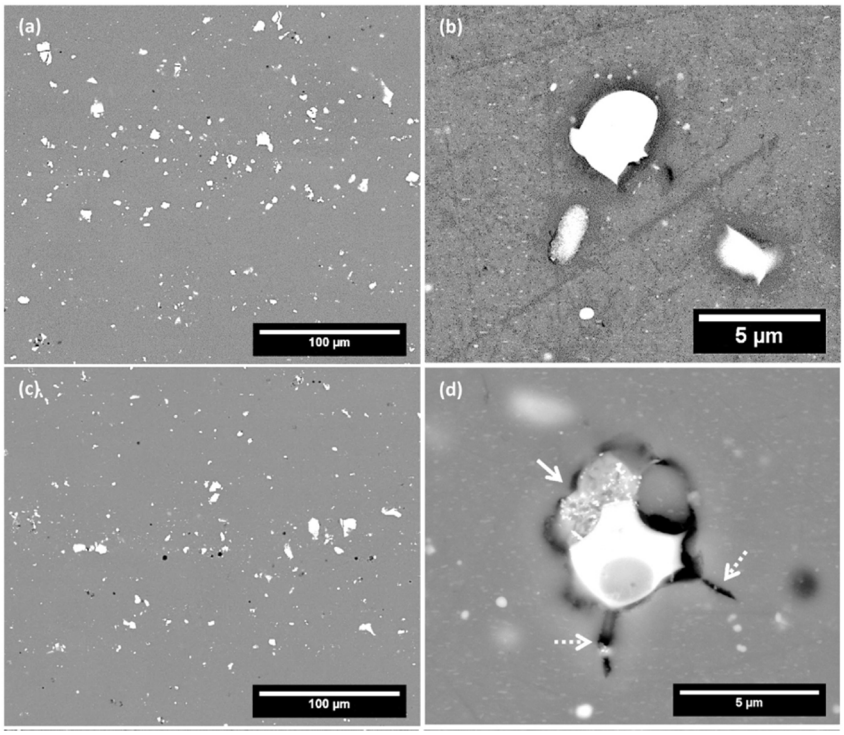

Figure 6. SEM micrographs of surface morphology of AA2024 alloy after anodic polarization to the various stages indicated in Figure 5: (**a**,**b**) surface morphology at stage 1; (**c**,**d**) surface morphology at stage 2 [27].

6. Surface Treatment

Conversion coating is often employed in the metal finishing industry as a pre-treatment layer to provide the final corrosion-protective barrier in the case that the coating system is completely damaged. It involves conversion of part of the substrate surface into the coating by means of a chemical or electrochemical process, e.g., anodizing and chromate conversion treatment. The coating thickness can range from several nanometers to hundreds of nanometers.

In Figure 7, the structure of a typical coating system on an Al alloy is schematically illustrated, which normally consists of three coating layers [25]. The innermost layer is formed by a pre-treatment (usually conversion coating) to improve the adhesion between the substrate and the primer and provide corrosion protection. As the principal corrosion-protective layer, the primer is composed of a pigmented organic resin matrix in the middle of the coating system. The top, decorative layer is paint with the ability to prevent corrosion of the materials. The principal conversion coatings used on Al alloys include chromate conversion coating (CCC), trivalent chromium process (TCP) coating and anodic film as shown in Table 2. With consideration of the complex structure in sports equipment, conversion coatings were employed first for the surface treatment on aluminum alloy. In this paper, we focused on the advances of research and application of chemical conversion coatings.

6.1. Chromate Conversion Coating

Chromate conversion coatings (CCCs) are primarily used as a primer, corrosion inhibitor and decorative finish. It has been more than ninety years since Bauer and Vogel formed this protective conversion coating on aluminum alloys in dichromate-based solution in 1915 [28]. A comprehensive understanding of the composition and corrosion-protective mechanisms of CCCs has been obtained in the last twenty years or so. The coatings are regarded as the most effective and common coating system so far for aluminum and its

alloys. It is due to the carcinogenetic toxicity of Cr(VI) that alternatives with environment-friendly and equally corrosion-protective properties are studied extensively.

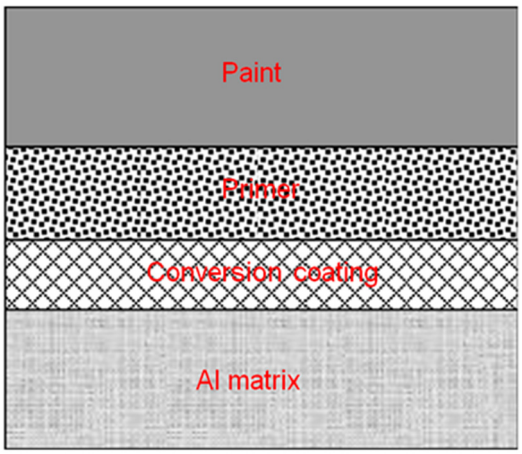

Figure 7. Schematic illustration of typical coating system on Al matrix [25].

Table 2. Types of surface treatment applied on aluminum alloys.

Types	Features
Chemical conversion coatings	No electrocity input; high economic efficiency; strong operability; coating thickness ranging from 10 nm to 100 μm.
Electroplating	The coating thickness can be controlled over a large range, with the least amount of metal used for the coating, without the need for heating or low temperature. The purity of the coating is high, and it firmly adheres to the surface of the plated part. The coating thickness is relatively uniform.
Anodizing film	The film generated by anodizing ranges from a few micrometers to several tens of micrometers and is hard and wear-resistant; the film generated by conductive oxidation is only 0.01–0.15 microns, and its wear resistance is not very good, but it can conduct electricity and resist atmospheric corrosion.

It is generally accepted that the nature of CCC formation is a chemical or electrochemical process on aluminum and its alloys [29–31]. On pure aluminum, Brown et al. [29–31] have studied CCC development in typical chromate/fluoride solutions. They found that the initial sites for CCCs are flaw sites on the surface, e.g., dislocations and grain boundaries. They are cathodic with respect to the surrounding anodic matrix because of the impurity accumulation at these flaw sites. They developed the overall cell reaction for CCC growth as follows:

$$2Al^0 + Cr_2O_7^{2-} + 2H^+ + 6HF \rightarrow 2AlF_3(soluble) + Cr_2O_3 \cdot H_2O + 3H_2O \quad (1)$$

Between the pre-existing metal ridges, the fluoride-containing acid solution chemically removes the initial oxide film, resulting in a dynamic equilibrium between alumina film growth and its dissolution. Consequently, local scalloping forms at the metal/conversion coating interface because of the transport of Al^{3+} ions from the surface into the solution.

In terms of the composition and morphology, Kim et al. [28] suggested that CCCs on pure Al are primarily composed of chromium-containing material, probably hydrated chromic oxide with a small amount of included dichromate anion. The amorphous and cellular-like structures were essentially investigated, in which aluminum and fluoride penetrated into the intercellular regions, probably in the form of a complex oxyfluoride.

For aluminum alloys, it is well-accepted that the formation of CCCs on Al alloys is via a redox reaction between chromate species in solution and component parts of alloys, e.g., IMCs and aluminum matrix. Thus, the following is suggested as the overall CCC reaction in chromate/fluoride solutions:

$$Cr_2O_7^{2-} + 2Al^0 + 2H^+ + H_2O \rightarrow 2CrOOH\downarrow + 2AlOOH\downarrow \quad (2)$$

The presence of HF facilitates the dissolution of a thin air-formed film to activate the alloy surface to permit nucleation and lateral growth of the conversion coating and also helps dissolve the AlOOH to promote the continuous reaction of chromate species at the Al interface above [32].

The mechanism of CCC formation on an Al alloy is made more complex owing to dissimilarities of surface composition and reactivity between constituent particles and matrix. For the initial growth of CCCs on AA2024-T3, Kunlinich et al. [33] found evidence to support the notion that the CCC process is electrochemical in nature and suggested that the reduction of Cr(VI) to Cr(III) begins on the Al-Cu-Fe-Mn IMCs, which act as cathodic sites, and then over the entire Al matrix surface. The function of processing time and environmental exposure was investigated by Kendig et al. [34], and they suggested the major constituent of CCCs on Al and its alloys is Cr(VI) (the ratio of Cr(VI):Cr(III) is approximately 4:1) and the Cr(III) is not crystalline Cr_2O_3 but has a closer resemblance to an amorphous hydrated $Cr(OH)_3$. In addition, there exists a limit for both the total amount of chromium and the ratio of Cr(VI):Cr(III) in CCCs after about 5 min of processing.

A so-called sol–gel mechanism, as a newer interpretation of CCC formation on Al, has been proposed [34,35]. It was suggested that there are three steps for coating formation, that is, hydrolysis, polymerization and condensation of Cr^{3+} (Figure 8). During the reaction process, Cr^{6+} species are reduced at the metal surface and hydrogen reduction leads to near-surface pH increases on the activated Al surface. In the consequent coatings, a chromium hydroxide ($Cr(OH)_3$) polymer "backbone" consists of edge- and corner-sharing Cr^{3+} octahedral units. The labile Cr^{6+} reservoir builds up in the coating simultaneously with backbone formation. It was suggested that the freshly formed conversion coating is a well-hydrated gel within the first 24 h after coating application. The gel coating becomes decreasingly receptive to organic overcoats, after aging for more than 24 h. The hardening CCCs can be used for stand-alone corrosion protection at that time.

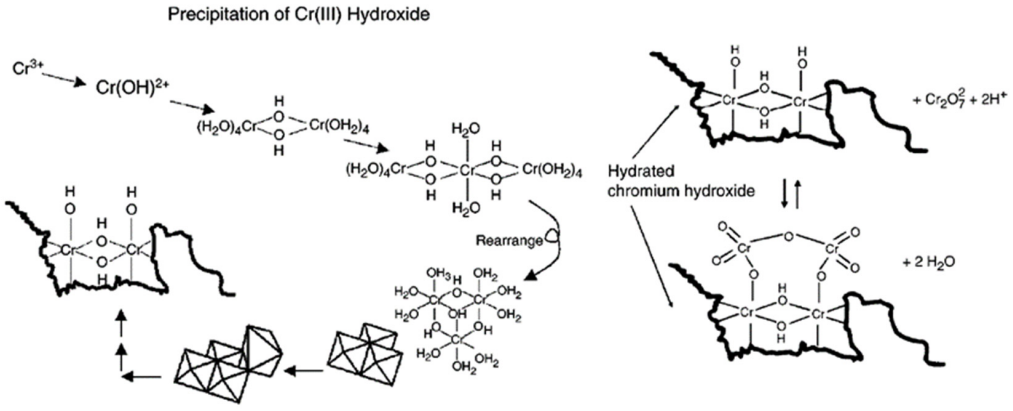

Figure 8. Schematic representation of the hydrolysis–polymerization–precipitation mechanism for $Cr(OH)_3$ backbone formation [36].

In addition, Figure 9 shows the scanning electron microscopy observations of the fracture surfaces of the deoxidized well-coated samples after fatigue tests. The fatigue life of the deoxidized and coated samples is significantly shorter at medium stress levels, which indicates a change in the point of crack initiation [37].

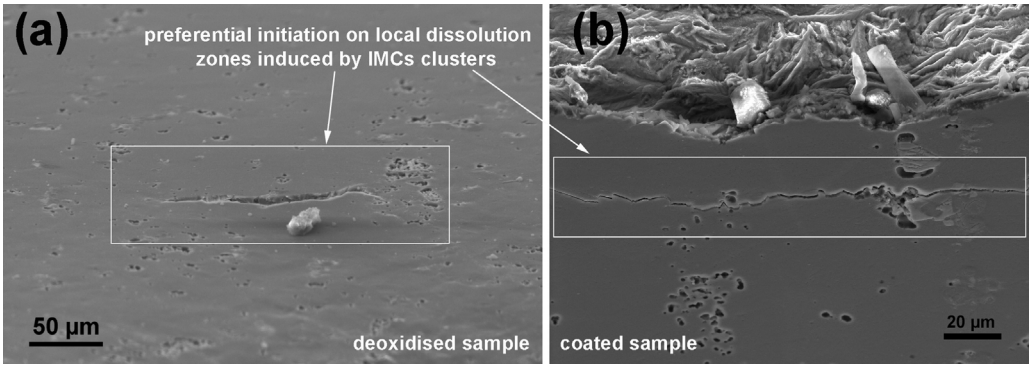

Figure 9. Fracture surface observations by SEM of deoxidized (**a**) and coated (**b**) AA 2024-T3 after fatigue tests [37].

Researchers have developed different models in recent decades to facilitate a better understanding of the morphology and composition of CCCs on individual IMCs and on the entire AA 2024-T3 alloy surface [34–42]. For instance, Hughes et al. [38] illustrated the structures of CCCs as shown in Figure 10, in which the external layer is composed of CrOOH, with a significant level of $Fe(CN)_6^{3-}$ and small amounts of chromate species. A mixture of Cr_2O_3·CrOOH, F^- and $Fe(CN)_6^{3-}$ anions makes up the bulk coatings and the interface between the bulk coating and substrate contains (Cr, Al)OF, Al_2O_3 and Cu. In Figure 11, it is shown that Vasquez [4] developed a new compositional model for the CCC, which suggests the following: (1) the CCC is of chemically and topographically heterogeneous composition; (2) the CCC composition varies laterally with the distribution and morphology of the IMCs in the alloy substrate; (3) a thinner CCC is formed on Cu-enriched particles due to ferrricyanide being absorbed and retained on these IMCs and the lack of Al availability; (4) the chromate of the CCC on the regions over the Cu-rich IMCs is not available for repair.

The CCCs are remarkable for this "self-healing" ability, that is, the soluble chromate species can transport and migrate to scratch sites to repair defects and damage of the conversion coating when exposed to a corrosive environment [43]. Frankel [43–48] investigated the mechanism of chromates and CCCs against corrosion and gave a number of specific working hypotheses. Cr^{6+} oxoanions have the following roles:

- being highly soluble and very mobile in solution, migrating to the vicinity of localized corrosion where they are reduced to Cr^{3+} and irreversibly adsorb at metal surfaces where they inhibit oxygen reduction;
- inhibiting pit initiation of Al and dissolution of active IMCs in Al alloys;
- modifying the chemical composition of surface of passive oxides and passivating IMCs by adsorption and buffering;
- lowering the zeta potential by adsorption on Al oxides, thus halting adsorption of corrosive anions such as chloride.

CCCs:

- are a good, hydrophobic Cr^{3+} hydroxide barrier with adhesion-promoting chemical and mechanical properties;
- not only contain Cr^{6+} oxoanions but also provide a continuous timed-release source into an aggressive solution and then migrate to repair defects to inhibit corrosion;
- inhibit anodic and cathodic reactions, at least temporarily, resulting in corrosion protection.

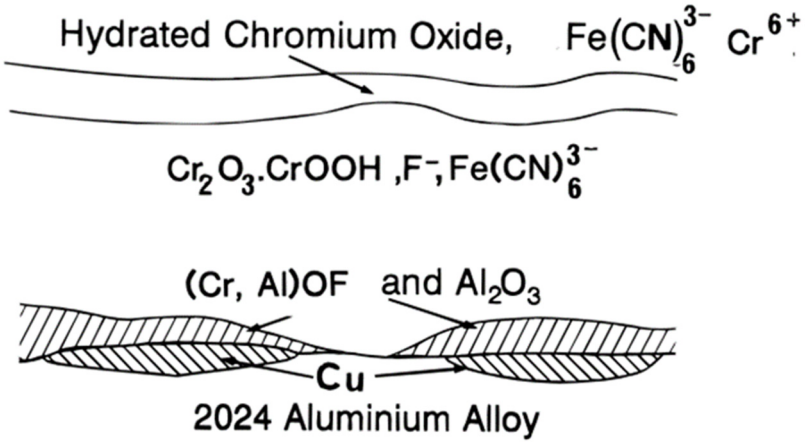

Figure 10. Illustration model for the chromate conversion coating formed on AA 2024-T3 [38].

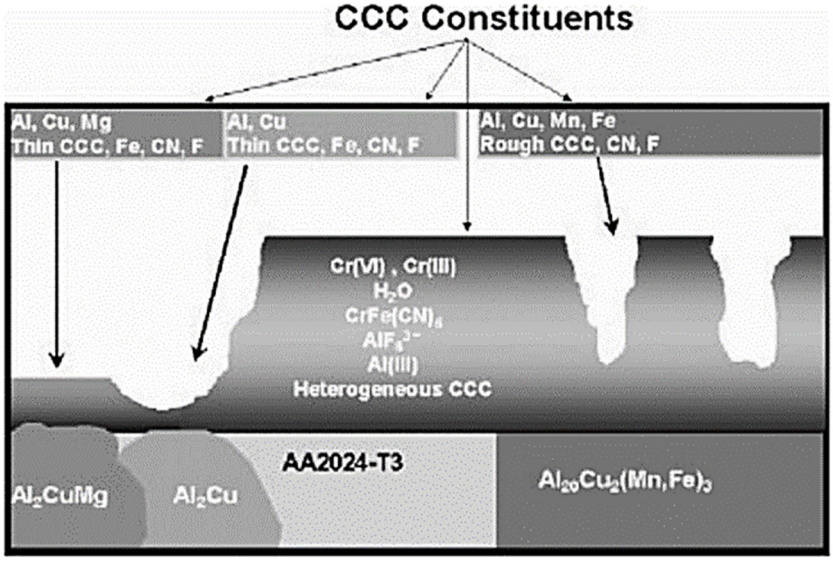

Figure 11. Refined model for the CCC formed on AA 2024-T3 alloy [39].

Akiyama et al. [49] extensively investigated the release of chromate ions from CCC on aluminum alloys by UV–visible spectroscopy and the effect of CCC aging on chromate release in order to facilitate optimum corrosion protection. They suggested that heat treatment and increasing aging time at room temperature can decrease the chromate release rate and proposed a diffusion-control model, resulting in a concentration gradient of soluble Cr(VI) as the chromate is released.

6.2. Trivalent Chromium Conversion (TCC)

TCC coating solution contains trivalent chromium sulfate, sodium hexafluoroalkanoate, sodium fluoride and other additives, and the recommended pH value for film.

formation is 3.8–4.0 and the temperature is 40 °C [4]. The formation mechanism of trivalent chromium conversion (TCC) coatings is a pH-driven reaction of trivalent chromium at the solution–metal interface to produce chromium/zirconium hydroxide deposits. They are the main components of the coatings. Figure 12 shows the polarization curve of electropolished aluminum in SurTec 650 solution (40 °C, pH 3.9), with a scan from −2.0 VSCE to 0 VSCE, where the polarization curve is affected by cathodic polarization, with lower potentials in the polarization curve where the current density is zero [50]. Sun et al. compared the interfacial pH evolution of aluminum and its alloys with that of magnesium alloys during the formation of TCC coatings and discussed the pH-based coating formation mechanism. The peak and final pH values of pre-treated Al, AA 2024

and AZ91D alloys were 4.9 and 3.5, 4.3, 4.1, 4.7 and 3.5, respectively. The changes in the interfacial pH were related to the hydrolysis of the weakly acidic nature of the zirconium and chromium salts, which are the main constituents of the TCC coating solutions [4].

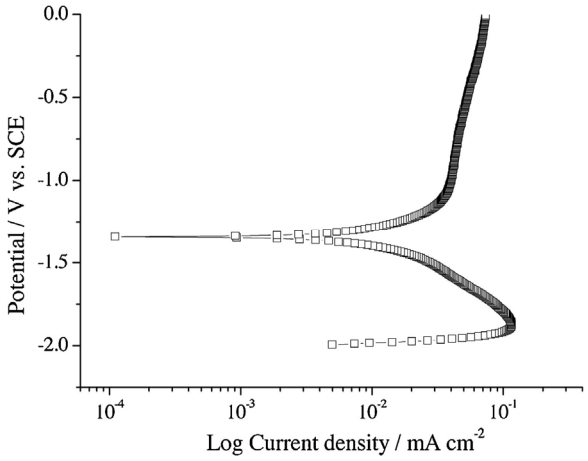

Figure 12. Potentiodynamic polarization curve of electropolished aluminum during immersion in SurTec 650 chromitAL solution (40 °C, pH 3.9) for 2000s [50].

7. Challenges and Prospects

CCCs are regarded as effective corrosion inhibitors on high-strength aluminum alloys. However, the use of Cr(VI) is tightly regulated by environmental requirements due to a toxic and carcinogenic risk to human beings and the environment. Underlying studies find that the static presence of Cr^{3+} or Cr^{6+} cannot directly contribute to DNA damage, leading to cancer [44,51,52]. Indeed, critical damage to DNA is induced by molecular fragmentation associated with the process of reduction of Cr(IV) to Cr(III) [44,51,52]. Thus, there has been a high focus in recent years on promising alternative and less toxic conversion coatings that offer equally effective corrosion-protective properties as CCCs.

Kendig and Buchheit [43] reviewed the considerable efforts, suggested alternatives for chromium element were considered from the periodic table, and the inorganic species were categorized as follows:

- reducible hypervalent transition metals (mixtures of Mo, V, Mn, Tc), like Cr, being highly soluble and mobile due to their high-valent oxoanions in aqueous solution. The results of Qian et al. showed that Mo-Zr-Ti composite conversion coating improves the corrosion resistance of LY12 aluminum alloy [53,54]. Compared with the Al alloy matrix, the MoTiZrCC surface under the optimal transformation parameters is more uniform and denser. In the meantime, the interstitial space related to corrosion resistance basically disappears, so the corrosion resistance of the alloy is improved by nearly six times [55].
- noble transition metal oxides (Zr, Hf, Ta, Ti, Y) and covalent oxides (oxides and mixed oxides of Si, Ge, P, Te), all processed by means of sol–gel chemistry. Among them, Ti/Zr/Mo composite conversion coatings, zirconium conversion coatings and titanium–zinc-based conversion coatings have been applied to improve the corrosion resistance of aluminum alloys, for example, to improve the corrosion resistance of outdoor fitness equipment [55–57].
- precipitated coatings as a type of barrier layer (boehmite and hydrotalcite coatings) and rare-earth metal (REM) used as "drop-in" methods. For example, nano-oxide-decorated nickel–aluminum–polyvanadate layered double hydroxides and the replacement of Mg-Al layered double hydroxides with Ce can improve the corrosion protection of aluminum alloys and thus prolong their life span [58–60].

For the future trends, self-organizing chemistries and biomemetic technologies, advances in the development of smart, self-diagnosing corrosion-protective coatings present

a fruitful area of research effort. In the past, pharmaceutical companies have used combinational methods to synthesize and screen classes of chemical methods for a particular drug application. Thus, it may be an appropriate methodology to discover an effective corrosion inhibitor of key aerospace alloys [43].

Kulinich and Akhtar [52] also indicated that the increasing research on Cr(VI)-free coatings includes stand-alone chemistry and combinations for organosilane-based chemistries, electroactive polymers, sol–gel coatings and inorganic conversion coating systems. A number of such non-chromate coatings exhibit similar performance to CrCCs under certain conditions, and the problems of formation and large-scale processing details require much study in the future. Thus, extensive studies should focus on comparisons between the various candidate coatings (combination of theory and mechanism) and those based on chromates. Among the various alternatives for CrCCs, the trivalent conversion coatings are well-accepted promising candidates within low toxicity and similarity to CrCCs. However, a concern is to optimize the corrosion-protective properties to reach the level of CrCCs.

In terms of the chromate electroplating process, the closed-loop system has been widely employed in the European Union and United States as reported in [61–63]. In comparison, this application is on the way in China such as at Northeast Electric Group High-voltage Switch Co., Ltd. The closed-loop system of chromate electroplating as the surface treatment of aluminum alloys is an eco-friendly, efficient and sustainable process. Chromate electroplating can provide good formability and corrosion-resistant performance and the toxic waste water and gas can be efficiently recycled [64]. Notably, 30% chromate acid mist could be generated during the conventional chromate electroplating process without the closed-loop system and such mist is toxic and carcinogenic to human beings [65]. The mist containing perfluorooctane sulfonate (PFOS) was widely used while PFOS is an organic pollutant that is highly limited by European POP Regulation (EC) No. 850/2004. In this sense, the closed-loop system of chromate electroplating is of great significance to the sustainable development of surface treatment of aluminum alloys.

8. Conclusions

Low-weight aluminum alloys are promising materials for sports equipment and second-phase particles create the risk of localized corrosion and result in the failure of sports equipment. Chromate conversion coatings were employed to provide a thin but compact film against corrosion and improve the binding property between alloys and outer paint. However, chromate species are regarded as toxic and carcinogenic chemicals for human beings. Thus, this process has been highly limited. Non-toxic TCCs, containing trivalent chromium, zirconium and titanium salts, have become the best surface treatment. In addition, the closed-loop system of the chromate electroplating process has been used in Europe and the United States. This is also a sustainable process for surface treatment of aluminum alloys applied in sports equipment.

Author Contributions: Investigation, writing—original draft preparation: B.L.; validation, resources: Y.X.; investigation, and writing—review and editing: J.L.; supervision, management: J.Q.; supervision: A.Y.; supervision, management: Q.Z. All authors have read and agreed to the published version of the manuscript.

Funding: This work is supported by Innovation and Entrepreneurship Project for College Students by China University of Petroleum (East China) (202210425055, 20190363), Shandong Natural Science Foundation (ZR2017LEM005), the University-Industry Collaborative Education Program of MOE in China (BINTECH-KJZX-20220831-35), Ministry of Education Industry-University Cooperation Collaborative Education Program (230802897074113) and Ministry of Education Industry-University Cooperation Collaborative Education Program (230804643073508).

Data Availability Statement: No new data were created or analyzed in this study. Data sharing is not applicable to this article.

Acknowledgments: Thanks to the above funds.

Conflicts of Interest: The authors declare no conflicts of interest.

References

1. Linthorne, N. Design and Materials in Athletics. In *Materials in Sports Equipment*; Woodhead Publishing: Sawston, UK, 2007; pp. 296–320.
2. Chen, J. Surface engineered light alloys for sports equipment. In *Surface Engineering of Light Alloys*; Woodhead Publishing: Sawston, UK, 2010; pp. 549–567.
3. Subic, A.; Mouritz, A.; Troynikov, O. Sustainable design and environmental impact of materials in sports products. *Sports Technol.* **2009**, *2*, 67–79. [CrossRef]
4. Sun, W.; Bian, G.; Jia, L.; Pai, J.; Ye, Z.; Wang, N.; Qi, J.; Li, T. Study of Trivalent Chromium Conversion Coating Formation at Solution—Metal Interface. *Metals* **2023**, *13*, 93. [CrossRef]
5. Zhao, Q.; Liu, X.; Wang, H.; Zhu, Y.; An, Y.; Yu, D.; Qi, J. Research Progress in Corrosion Protection Technology for Electronic Components. *Metals* **2023**, *13*, 1508. [CrossRef]
6. Walker, A.; Subic, A. Advances in design and materials for indoor sports surfaces. *Adv. Mater. Res.* **2013**, *633*, 47–61. [CrossRef]
7. Yang, Y.; Kushima, A.; Han, W.; Xin, H.L.; Li, J. Liquid-like, self-healing aluminum oxide during deformation at room temperature. *Nano Lett.* **2018**, *18*, 2492–2497. [CrossRef] [PubMed]
8. Wang, Z. Application of aluminium in sports equipment. *Alum. Fabr.* **2017**, *10*, 1–5.
9. Huang, Y.; Jiang, J. Microstructure and texture evolution during severe plastic deformation at cryogenic temperatures in an Al-0.1Mg alloy. *Metals* **2021**, *11*, 1822. [CrossRef]
10. Oberreiter, M.; Pomberger, S.; Leitner, M.; Stoschka, M. Validation study on the statistical size effect in cast aluminium. *Metals* **2020**, *10*, 710. [CrossRef]
11. Gruber, R.; Singewald, T.D.; Bruckner, T.M.; Hader-Kregl, L.; Hafner, M.; Groiss, H.; Duchoslav, J.; Stifter, D. Investigation of oxide thickness on technical aluminium alloys—A comparison of characterization methods. *Metals* **2023**, *13*, 1322. [CrossRef]
12. Kaushik, N.C.; Rao, R.N. Effect of grit size on two body abrasive wear of Al 6082 hybrid composites produced by stir casting method. *Tribol. Int.* **2016**, *102*, 52–60. [CrossRef]
13. Buchheit, R.G.; Grant, R.P.; Hlava, P.F.; Mckenzie, B.; Zender, G.L. Local dissolution phenomena associated with S phase (Al_2CuMg) particles in aluminum alloy 2024-T3. *J. Electrochem. Soc.* **1997**, *144*, 2621–2628. [CrossRef]
14. Chen, G.S.; Gao, M.; Wei, R.P. microconstituent-induced pitting corrosion in aluminum alloy 2024-T3. *Corrosion* **1996**, *52*, 8–15. [CrossRef]
15. Hughes, A.E.; MacRae, C.; Wilson, N.; Torpy, A.; Muster, T.H.; Glenn, A.M. Sheet AA2024-T3: A new investigation of microstructure and composition. *Surf. Interface Anal.* **2010**, *42*, 334–338. [CrossRef]
16. Boag, A.; Hughes, A.E.; Wilson, N.C.; Torpy, A.; MacRae, C.M.; Glenn, A.M.; Muster, T.H. How complex is the microstructure of AA2024-T3? *Corros. Sci.* **2009**, *51*, 1565. [CrossRef]
17. Campestrini, P.; van Westing, E.; van Rooijen, H.; de Wit, J. Relation between microstructural aspects of AA2024 and its corrosion behaviour investigated using AFM scanning potential technique. *Corros. Sci.* **2000**, *42*, 1853–1861. [CrossRef]
18. Knipling, K.E.; Seidman, D.N.; Dunand, D.C. Ambient- and high-temperature mechanical properties of isochronally aged Al-0.06Sc, Al-0.06Zr and Al-0.06Sc-0.06Zr (at.%) alloys. *Acta Mater.* **2011**, *59*, 943. [CrossRef]
19. Wang, J.; Liu, J.; Wang, X. The anticorrosive applications of anionic surfactant on AA2024-T3 aluminum alloy in alkaline medium: Experimental and theory. *J. Mol. Struct.* **2023**, *1275*, 134612. [CrossRef]
20. Zupanič, F.; Steinacher, M.; Žist, S.; Bončina, T. Microstructure and properties of a novel Al-Mg-Si alloy aa 6086. *Metals* **2021**, *11*, 368. [CrossRef]
21. Ringer, S.P.; Sakurai, T.; Polmear, I.J. Origins of hardening in aged AlGuMg(Ag) alloys. *Acta Mater.* **1997**, *45*, 3731. [CrossRef]
22. Ozun, E.; Ceylan, R.; Bora, M.Ö.; Çoban, O.; Kutluk, T. Combined effect of surface pretreatment and nanomaterial reinforcement on the adhesion strength of aluminium joints. *Int. J. Adhes. Adhes.* **2022**, *119*, 103274. [CrossRef]
23. Snijders, P.C.; Jeurgens, L.P.H.; Sloof, W.G. Structure of thin aluminium-oxide films determined from valence band spectra measured using XPS. *Surf. Sci.* **2002**, *496*, 97. [CrossRef]
24. Hart, R.K. The formation of films on aluminium immersed in water. *Trans. Faraday Soc.* **1957**, *53*, 1020. [CrossRef]
25. Hughes, A.E.; Cole, I.S.; Muster, T.H.; Varley, R.J. Designing green, self-healing coatings for metal protection. *NPG Asia Mater.* **2010**, *2*, 143–151. [CrossRef]
26. Wei, W.; González, S.; Hashimoto, T.; Abuaisha, R.R.; Thompson, G.E.; Zhou, X. In-service sensitization of a micro-structurally heterogeneous AA5083 alloy. *Mater. Corros.* **2016**, *67*, 378–386. [CrossRef]
27. Zhang, X.; Zhou, X.; Hashimoto, T.; Liu, B. Localized corrosion in AA2024-T351 al-uminium alloy: Transition from intergranular corrosion to crystallographic pitting. *Mater. Charact.* **2017**, *130*, 230–236. [CrossRef]
28. Kim, M.; Brewer, L.N.; Kubacki, G.W. Microstructure and corrosion resistance of chromate conversion coating on cold sprayed aluminum alloy 2024. *Surf. Coatings Technol.* **2023**, *460*, 129423. [CrossRef]
29. Brown, G.; Shimizu, K.; Kobayashi, K.; Thompson, G.; Wood, G. The growth of chromate conversion coatings on high purity aluminium. *Corros. Sci.* **1993**, *34*, 1045–1054. [CrossRef]
30. Brown, G.; Shimizu, K.; Kobayashi, K.; Thompson, G.; Wood, G. The morphology, structure and mechanism of growth of chemical conversion coatings on aluminium. *Corros. Sci.* **1992**, *33*, 1371–1385. [CrossRef]

31. Brown, G.; Shimizu, K.; Kobayashi, K.; Thompson, G.; Wood, G. The development of chemical conversion coatings on aluminium. *Corros. Sci.* **1993**, *35*, 253–256. [CrossRef]
32. Katzman, H.A.; Malouf, G.M.; Bauer, R.; Stupian, G.W. Corrosion-protective chromate coatings on aluminum. *Appl. Surf. Sci.* **1979**, *2*, 416–432. [CrossRef]
33. Kulinich, S.A.; Akhtar, A.S.; Susac, D.; Wong, P.C.; Wong, K.C.; Mitchell, K.A.R. On the growth of conversion chromate coatings on 2024-Al alloy. *Appl. Surf. Sci.* **2007**, *253*, 3144–3153. [CrossRef]
34. Kendig, M.W.; Davenport, A.J.; Isaacs, H.S. The mechanism of corrosion inhibition by chromate conversion coatings from x-ray absorption near edge spectroscopy (Xanes). *Corros. Sci.* **1993**, *34*, 41. [CrossRef]
35. Osborne, J.H. Observations on chromate conversion coatings from a sol–gel perspective. *Prog. Org. Coat.* **2001**, *41*, 280–286. [CrossRef]
36. Xia, L.; McCreery, R.L. Chemistry of a chromate conversion coating on aluminum alloy AA2024-T3 probed by vibrational spectroscopy. *J. Electrochem. Soc.* **1998**, *145*, 3083. [CrossRef]
37. Akanou, M.; Saillard, R.; Fori, B.; Blanc, C.; Odemer, G. Effect of trivalent chromium process on fatigue lifetime of 2024-T3 aluminium alloy. *Mater. Sci. Eng. A* **2019**, *743*, 322–326. [CrossRef]
38. Hughes, A.E.; Taylor, R.J.; Hinton, B.R.W. Chromate conversion coatings on 2024 Al alloy. *Surf. Interface Anal.* **1997**, *25*, 223–234. [CrossRef]
39. Vasquez, M.J.; Halada, G.P.; Clayton, C.R.; Longtin, J.P. On the nature of the chromate conversion coating formed on intermetallic constituents of AA2024-T3. *Surf. Interface Anal.* **2002**, *33*, 607–616. [CrossRef]
40. Campestrini, P.; Goeminne, G.; Terryn, H.; Vereecken, J.; De Wit, J.H.W. Chromate conversion coating on aluminum alloys–I. *Formation mechanism J. Electrochem. Soc.* **2004**, *151*, B59–B80. [CrossRef]
41. Campestrini, P.; Goeminne, G.; Terryn, H.; Vereecken, J.; De Wit, J.H.W. Chromate conversion coating on aluminum alloys–II: Effect of the microstructure. *J. Electrochem. Soc.* **2004**, *151*, B369. [CrossRef]
42. Brown, G.M.; Kobayashi, K. Nucleation and growth of a chromate conversion coating on aluminum alloy AA 2024-T3. *J. Electrochem. Soc.* **2001**, *148*, B457–B466. [CrossRef]
43. Kinding, M.W.; Buchheit, R.G. Corrosion inhibition of aluminum and aluminum alloys by soluble chromates, chromate coatings, and chromate-free coatings. *Corrosion* **2003**, *59*, 379–400.
44. Frankel, G.S. *Mechanism of Al Alloy Corrosion and the Role of Chromate Inhibitors*; First Annual Report, Contract No. F49620-96-1-0479; Ohio State University: Columbus, OH, USA, 1997.
45. Frankel, G.S. *Mechanism of Al Alloy Corrosion and the Role of Chromate Inhibitors*; Second Annual Report, Contract No. F49620-96-1-0479; Ohio State University: Columbus, OH, USA, 1998.
46. Frankel, G.S. *Mechanism of Al Alloy Corrosion and the Role of Chromate Inhibitors*; Third Annual Report, Contract No. F49620-96-1-0479; Ohio State University: Columbus, OH, USA, 1999.
47. Frankel, G.S. *Mechanism of Al Alloy Corrosion and the Role of Chromate Inhibitors*; Fourth Annual Report, Contract No. F49620-96-1-0479; Ohio State University: Columbus, OH, USA, 2000.
48. Frankel, G.S. *Mechanism of Al Alloy Corrosion and the Role of Chromate Inhibitors*; Final Report, Contract No. F49620-96-1-0479; Ohio State University: Columbus, OH, USA, 2001.
49. Akiyama, E.; Markworth, A.J.; McCoy, J.K.; Frankel, G.S.; Xia, L.; McCreery, R.L. Storage and release of soluble hexavalent chromium from chromate conversion coatings–Equilibrium aspects of Cr-VI concentration. *J. Electrochem. Soc.* **2003**, *150*, B83. [CrossRef]
50. Qi, J.; Swiatowska, J.; Skeldon, P.; Marcus, P. Chromium valence change in trivalent chromium conversion coatings on alu-minium deposited under applied potentials. *Corros. Sci.* **2020**, *167*, 108482. [CrossRef]
51. O'Brien, P.; Kortenkamp, A. The chemistry underlying chromate toxicity. *Transit. Met. Chem.* **1995**, *20*, 636–642. [CrossRef]
52. Kulinich, S.A.; Akhtar, A.S. On conversion coating treatments to replace chromating for Al alloys: Recent developments and possible future directions. *Russ. J. Non-Ferr. Metals* **2012**, *53*, 176. [CrossRef]
53. Qian, X.; Zhan, W.; Pan, J.; Liu, Y.; Huang, F.; Wang, B. Improving the corrosion resistance of LY12 aluminum alloy via a novel Mo–Zr–Ti composite conversion coating. *Mater. Res. Express* **2021**, *8*, 036403. [CrossRef]
54. Qian, X.; Huang, F.; Teng, X.; Wang, Y.; Fang, Y.; Pan, J.; Wang, W.; Li, Y.; Zhan, W. The Preparation, Corrosion Resistance and Formation Mechanism of a New-Type Mo-Based Composite Conversion Coating on 6061 Aluminum Alloy. *Metals* **2023**, *13*, 168. [CrossRef]
55. Wang, Y.; Qian, X.; Huang, F.; Fan, Y.; Wang, T.; Hu, L. Improving the anticorrosion property of outdoor fitness equipment via a novel Ti/Zr/Mo composite conversion coating. *Mater. Res. Express* **2023**, *10*, 076403. [CrossRef]
56. Šekularac, G.; Milošev, I. Electrochemical behavior and Self-Sealing ability of zirconium conversion coating applied on aluminum Alloy 3005 in 0.5 M NaCl Solution. *J. Electrochem. Soc.* **2020**, *167*, 021509. [CrossRef]
57. Zhang, H.; Zhang, X.; Zhao, X.; Tang, Y.; Zuo, Y. Preparation of Ti–Zr-based conversion coating on 5052 Aluminum alloy, and its corrosion resistance and antifouling performance. *Coatings* **2018**, *8*, 397. [CrossRef]
58. Pancrecious, J.K.; Vineetha, S.V.; Bill, U.S.; Gowd, E.B.; Rajan, T.P.D. Ni-Al polyvanadate layered double hydroxide with nanoceria decoration for enhanced corrosion protection of aluminium alloy. *Appl. Clay Sci.* **2021**, *211*, 106199. [CrossRef]
59. Vieira, D.E.; Salak, A.N.; Ferreira, M.G.; Vieira, J.M.; Brett, C.M. Ce-substituted Mg-Al layered double hydroxides to prolong the corrosion protection lifetime of aluminium alloys. *Appl. Surf. Sci.* **2022**, *573*, 151527. [CrossRef]

60. Wu, G.; Wang, C.; Zhang, Q.; Kang, P. Characterization of Ce conversion coating on Gr-f/6061Al composite surface for corrosion protection. *J. Alloys Compd.* **2008**, *461*, 389–394. [CrossRef]
61. Munsamy, M.; Telukdarie, A.; Zhang, W. Cleaner technology systems for surface finishing: Evaporative coolers for close circuiting low temperature plating process. *J. Clean. Prod.* **2014**, *66*, 664–671. [CrossRef]
62. Leigh, M.; Li, X. Industrial ecology, industrial symbiosis and supply chain environmental sustainability: A case study of a large UK distributor. *J. Clean. Prod.* **2015**, *106*, 632–643. [CrossRef]
63. Scarazzato, T.; Panossian, Z.; Tenorio, J.A.S.; Pérez-Herranz, V.; Espinosa, D.C.R. A review of cleaner production in electroplating industries using electrodial ysis. *J. Clean. Prod.* **2017**, *168*, 1590–1602. [CrossRef]
64. Zhang, Z.; Zhang, J.; Zhao, X.; Cheng, X.; Jiang, S.; Zhang, Q. Effects of Al-Mg on the Microstructure and Phase Distribution of Zn-Al-Mg Coatings. *Metals* **2023**, *13*, 46. [CrossRef]
65. Chen, W.; Lu, W.; Gou, G.; Dian, L.; Zhu, Z.; Jin, J. The Effect of Fatigue Damage on the Corrosion Fatigue Crack Growth Mechanism in A7N01P-T4 Aluminum Alloy. *Metals* **2023**, *13*, 104. [CrossRef]